Analytical and Bioanalytical Chemistry
https://doi.org/10.1007/s00216-019-01739-9

RESEARCH PAPER

# Electrochemical DNA biosensors for label-free breast cancer gene marker detection

Mehmet Senel[1] · Muamer Dervisevic[2] · Firdevs Kokkokoğlu[3]

Received: 30 January 2019 / Revised: 21 February 2019 / Accepted: 28 February 2019


## Abstract

We present an electrochemical DNA detection strategy based on self-assembled ferrocene-cored poly(amidoamine) dendrimers for the detection of a gene relevant to breast cancer. The chemisorption of three ferrocene-cored poly(amidoamine) generations and hybridization of single-stranded DNA on a Au electrode were studied by cyclic voltammetry and differential pulse voltammetry. The biosensor demonstrated high sensitivity of 0.13 μA/(ng/ml) in the detection of the target DNA with a linear range of 1.3–20 nM and a detection limit of 0.38 nM. The DNA biosensor also has high selectivity for the target DNA, showing a clear signal difference from a noncomplementary sequence and a single-base-mismatch sequence, which was used as a model of *BRAC1* gene mutation. The results shown are highly motivating for exploring DNA biosensing technology in the diagnosis of breast cancer caused by mutation of the *BRAC1* gene.

**Keywords** Electrochemical DNA biosensor · Ferrocene · Poly(amidoamine) · Dendrimer · Breast cancer

## Introduction

DNA-biosensor-based diagnostics has attracted considerable attention because of simple nucleic acid hybridization and applicability in the detection of various diseases, such as tuberculosis [1], meningitis [2], lung cancer [3], and breast cancer [4–6]. Cancer is the second-leading cause of death worldwide, and was responsible for 9.6 million deaths in 2018 according to the World Health Organization [7]. Among all cancers, breast cancer is the most common cancer affecting women's health worldwide, with approximately two million breast cancer cases in 2018 according to the World Health Organization. It is estimated that more that 80% of inherited breast and ovarian cancers are caused by mutations in the tumor suppressor breast cancer type 1 susceptibility protein gene (*BRCA1*) [8, 9]. Mutations identified in the *BRAC1* gene involve deletions, inferred regulatory mutation, a missense substitution, and a one-pair insertion [10]. The breast cancer survival rate in developed countries is 80% or greater; however, in low-income countries the rate is below 40% [11], which is mainly due to the lack of early detection methods. Current diagnostic methods preformed in commercial laboratories are usually based on commercial kits that include DNA extraction, isolation, amplification, etc. [12], and the cost of testing can range from a few hundred dollars to a few thousand dollars. For this reason, the development of reliable and affordable technology for early diagnosis of breast cancer is in high demand.

Among the different types of DNA sensors and detection technologies, electrochemical DNA biosensors are particularly attractive because of their high sensitivity, simplicity, miniaturization, and low cost [4, 13]. These biosensors, at the molecular level, have elegant routes for interfacing, such as DNA recognition and signal-transduction events where DNA hybridization sensors rely on the conversion of the hybridization of the DNA probe and the target DNA into an electrical signal [13]. To obtain a useful electrical signal, chemical modification of the electrode surface has to be done carefully so that surface can be a suitable interface for the immobilization of the probe DNA. Furthermore, to increase signal intensity and sensitivity of the biosensors, different types of redox markers are incorporated in

✉ Mehmet Senel
msenel81@gmail.com

[1] SANKARA Brain & Biotechnology Research Center, Nanoyasam Nanobiotechnology Company, Technocity, Avcılar, 34320 Istanbul, Turkey

[2] Monash Institute of Pharmaceutical Sciences, Monash University, Parkville, VIC 3052, Australia

[3] Dabska 18H 52-571, Kraków, Poland

Published online: 08 April 2019

the immobilization matrix. One of the most familiar redox markers is ferrocene.

Ferrocene serves as a redox marker and electron-transfer mediator between the biological recognition element and the electrode surface. Ferrocene and its derivatives have been widely used in electrochemical biosensing because of their favorable characteristics, including low oxidation potential, stability in each redox state, and capacity for fast electron transfer [14–17], and have been applied in different DNA- and cancer-biomarker-based biosensors [18–20]. On the other hand, dendrimers, which cannot act as a redox marker, are highly branched globular-shaped structures with a diameter of 2–20 nm. Dendrimers are one of the most preferred synthetic macromolecules for biosensing because of their extraordinary characteristics, such as monodispersibility, controllable size and surface functional groups, hydrophilicity, and chemical and mechanical solidity [21, 22]. Synthesis of poly(amidoamine) (PAMAM) dendrimers was first reported in 1985 by Tomalia and his coworkers [23], where they had an ethylenediamine core and an amidoamine repeating monomer [22, 24]. The advantage of using these dendrimers in biosensing applications comes from the presence of covalently modifiable branches with biorecognition materials such as enzymes, aptamers, and nucleotide probes. PAMAM dendrimers are an excellent platform that has been successfully applied in DNA detection [25, 26], cancer detection [19, 27], and enzymatic biosensors [28–30]. Because of the high number of amine groups on the PAMAM surface, PAMAM can provide a larger amount of probe DNA immobilization, which can decrease the detection limit. Moreover, including ferrocene as a redox marker together with dendrimers can increase sensitivity and provide more persistent surface modification, leading to better reproducibility.

In this work, for first time we explore the application of three different ferrocene-cored PAMAM (Fc-PAMAM) generations in electrochemical DNA biosensing for breast cancer detection. The biosensor was fabricated by immobilization of single-stranded DNA (ssDNA) on self-assembled Fc-PAMAM by the bifunctional cross-linker glutaraldehyde. The electrode showed high selectivity toward target DNA and excellent differentiation of noncomplementary, single-base-mismatch, and target DNA sequences. The biosensor has a wide linear range

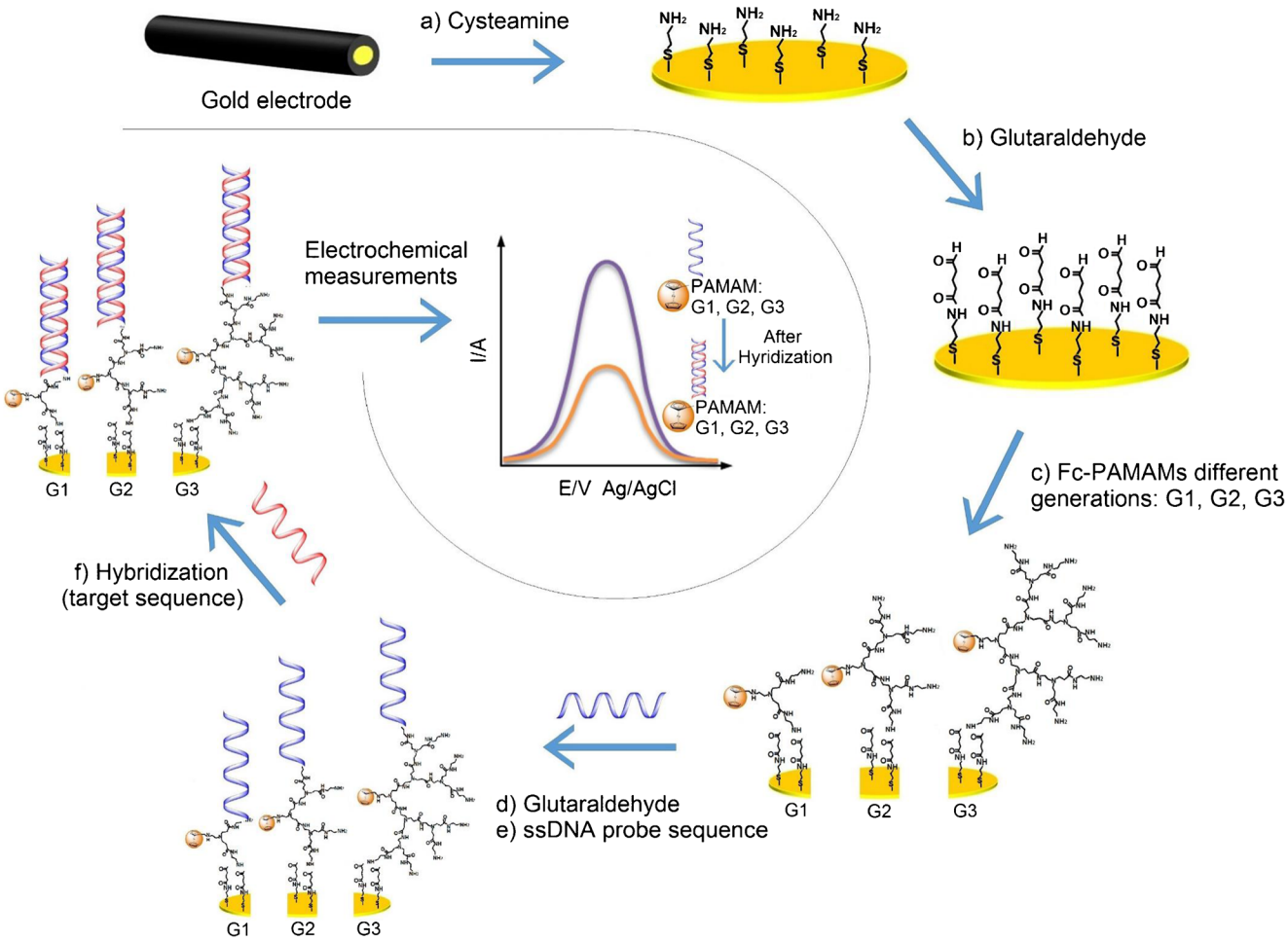


**Fig. 1** Preparation of the DNA biosensor based on three different generations of ferrocene (Fc)-cored poly(amidoamine) (PAMAM). G1 generation 1, G2 generation 2, G3 generation 3, ssDNA single-stranded DNA

of 10–150 ng DNA per milliliter (1.3–20 nM), a detection limit of 2.9 ng/ml (0.38 nM), and sensitivity of 0.13 μA/(ng/ml).

## Experimental

### Materials and instruments

Ferrocene carboxyaldehyde, cystaminium dichloride, and glutaraldehyde were purchased from Sigma-Aldrich, and methyl acrylate and ethylenediamine were purchased from Merck. The Fc-PAMAM dendrimers with different generations [generation 1 (G1), generation 2 (G2), and generation (G3)] were synthesized according to our previous study [31]. All other chemicals were of analytical grade and were used without further purification. All oligonucleotides were purchased from Alpha-DNA (USA or Canada).

The base sequences of the oligonucleotides studied are as follows:

Probe sequence (5′–3′) [$NH_2$] ATGGCTGCGTGTGA CGCGCTCAG
Target sequence (5′–3′) CTGAGCGCGTCACA CGCAGCCAT
One-point-mutation sequence: (5′–3′) CTG**G**GCGC GTCACACGCAGCCAT
Noncomplementary sequence: (5′–3′) AATACCTG TATTCCTCGCCTGTC

Electrochemical measurements were performed with a CHI 842B analyzer (CH Instruments) with a conventional three-

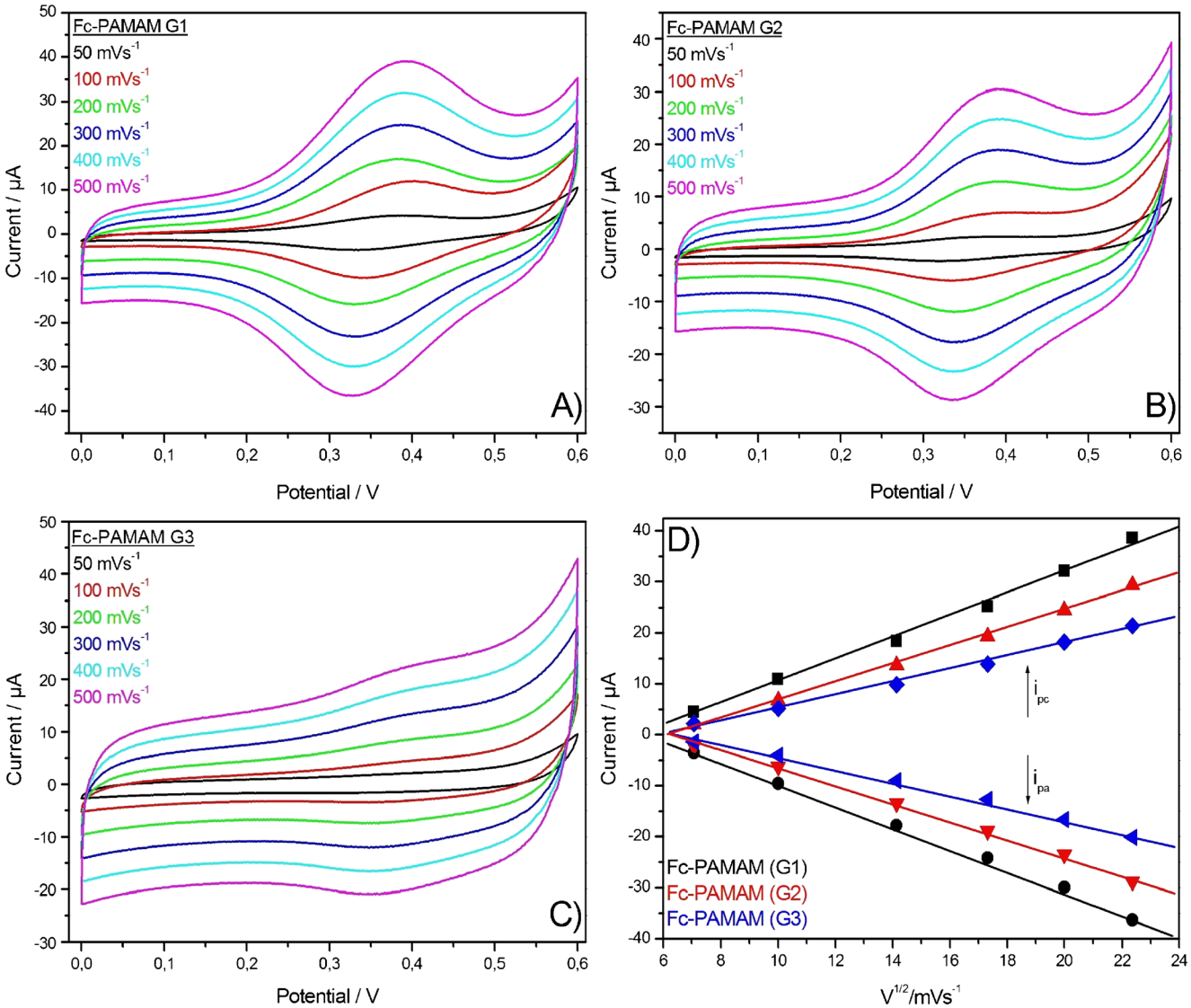


**Fig. 2** Cyclic voltammograms obtained with different scan rates (50–500 mV/s) of ferrocene-cored poly(amidoamine) (Fc-PAMAM) generations: **a** generation 1 (G1), **b** generation 2 (G2), and **c** generation 3 (G3). **d** Anodic and cathodic peak currents versus the square root of the scan rate

electrode electrochemical cell having a Au rod electrode as the working electrode, Pt as the counter electrode, and Ag/AgCl (saturated KCl) as the reference electrode, all purchased from CH Instruments.

## Preparation of the biosensor

### Modification of Au electrode surface

Before any modification, to remove any remaining impurities, the Au electrode (surface area of 0.031 $cm^2$) was polished with alumina powder, followed by washing with distilled water, 95% ethanol, and acetone. Electrochemical cleaning was performed by our etching the Au electrode in 0.5 mM $H_2SO_4$ solution by a cyclic voltammetry (CV) scan between −0.3 and 1.7 V until a reproducible voltammetric response was obtained. After cleaning, the electrode was immersed overnight in 20 mM cysteamine aqueous solution (Fig. 1a), and then it was thoroughly rinsed with distilled water to remove physically adsorbed cysteamine. Later, the electrode was immersed in 2.5% glutaraldehyde solution for 2 h (Fig. 1b), after which Fc-PAMAM modification was performed by our incubating the electrode in methanolic solution of 0.21 μM Fc-PAMAM dendrimers of three generations for 12 h at room temperature (Fig. 1c). Finally, electrodes were treated with 1% glutaraldehyde for 30 min before DNA immobilization.

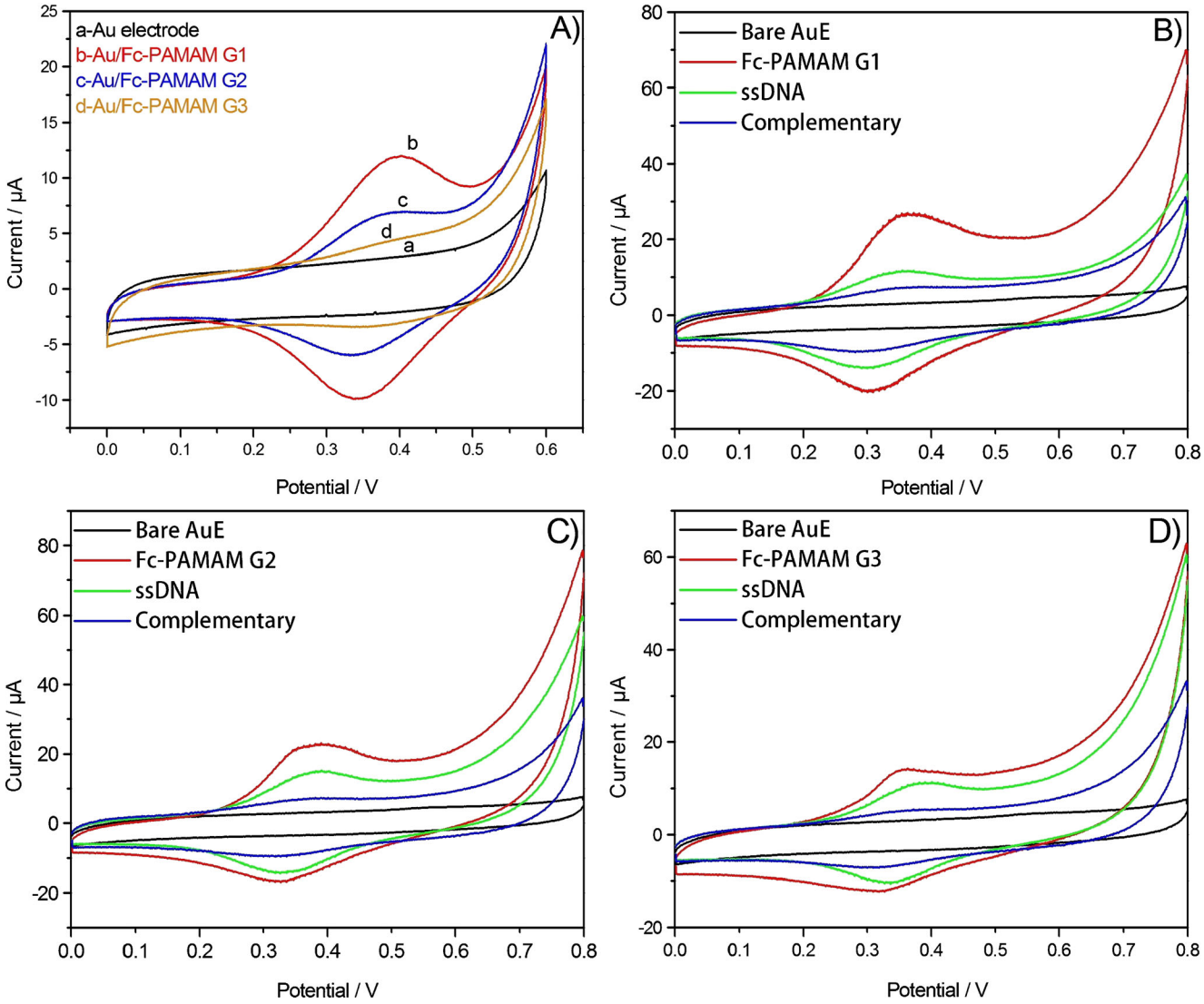


**Fig. 3** **a** Cyclic voltammetry comparison of different generations of ferrocene-cored poly(amidoamine) (Fc-PAMAM): Au electrode (a), generation 1 (G1) electrode (b), generation 2 (G2) electrode (c), and generation (G3) electrode (d) in 10 mM phosphate-buffered saline, pH 7.4, at 10 mV/s. Electrochemical characterization by cyclic voltammetry of Fc-PAMAM-modified electrodes: **b** G1, **c** G2, and **d** G3. Cyclic voltammograms of the bare Au electrode, Fc-PAMAM (G1, G2, G3), single-stranded DNA (ssDNA) probe, and complementary strand (target DNA) recorded at 100 mV/s are also shown. AuE Au electrode

### Immobilization of ssDNA and hybridization

The covalent immobilization of amine-modified complementary ssDNA sequences on the Fc-PAMAM-modified Au electrode (Au-Fc-PAMAM) was achieved by our drop casting glutaraldehyde (1%) and then leaving the electrode for 30 min at room temperature (Fig. 1d, e). Glutaraldehyde served as the linker between two amine groups: one from the dendrimers and the other from the ssDNA. The electrode was gently rinsed with ultrapure water, followed by our drop casting ssDNA on the active electrode surface and incubation for 1 h at room temperature. The fabricated electrode (Au-Fc-PAMAM/ssDNA) was ready to be used to analyze the interaction of immobilized complementary ssDNA with the target sequence. The hybridization was achieved by our incubating the Au-Fc-PAMAM/ssDNA electrode with the target ssDNA sequence for 1 h at room temperature (Fig. 1f). After hybridization, the biosensing electrode was once more gently rinsed with ultrapure water and was then used for the electrochemical measurements.

## Results and discussion

### Electrochemical characterization and optimization studies

The electrochemical properties of the biosensing electrode were analyzed by our recording the oxidation states and electron-transfer behavior under the effect of different scan rates in 10 mM phosphate-buffered saline, pH 7.4, in the potential range from 0.0 to 0.6 V. Figure 2 shows a series of CV scans of Fc-PAMAM G1 (Fig. 2a), Fc-PAMAM G2 (Fig. 2b), and Fc-PAMAM G3 (Fig. 2c) modified electrodes, recorded by our increasing the scan rate from 50 to 500 mV/s. The electrochemistry of Fc-PAMAM was dominated by one-electron reversible oxidation of the ferrocene nucleus. The oxidation peak illustrates the point where Fe(II) is oxidized to Fe(III), while the negative scan indicates the reduction of Fe(III). Further increase in the scan rate resulted in increase in both anodic and cathodic peak current, indicating a quasi-reversible process [19, 30]. The oxidation peak potential for Fc-PAMAM G1 was 0.4 V and the reduction peak potential was 0.33 V; for Fc-PAMAM G2 and Fc-PAMAM G3 the oxidation peak potential was 0.4 V and the reduction peak potential was 0.35 V. The higher the generation of the dendrimer, the further away the dendrimer keeps the ferrocene from the electrode surface, which results in a decrease in the intensity of the oxidation–reduction peaks. The results clearly illustrate that a dendrimer that extends from the electroactive ferrocene core tends to hinder the heterogeneous electron-transfer reactions of these dendrimers with the electrode. Figure 2d illustrates the cathodic and anodic linear relation of the peak currents obtained with increase of the square root of the scan rate ($V^{1/2}$). Linearity in $V^{1/2}$ indicates that charge propagation in the dendrimers occurs by a diffusion-like process, where electrons are hopping among neighboring redox sites and there is counterion motion. A linear correlation also confirms that the kinetics of the overall process was mainly controlled by the diffusion process.

CV scans of the electrodes modified with different Fc-PAMAM generations are shown in Fig. 3a. No reversible redox peaks corresponding to ferrocene were seen for the bare Au electrode. However, when Fc-PAMAM dendrimers were self-assembled on the Au electrode, a

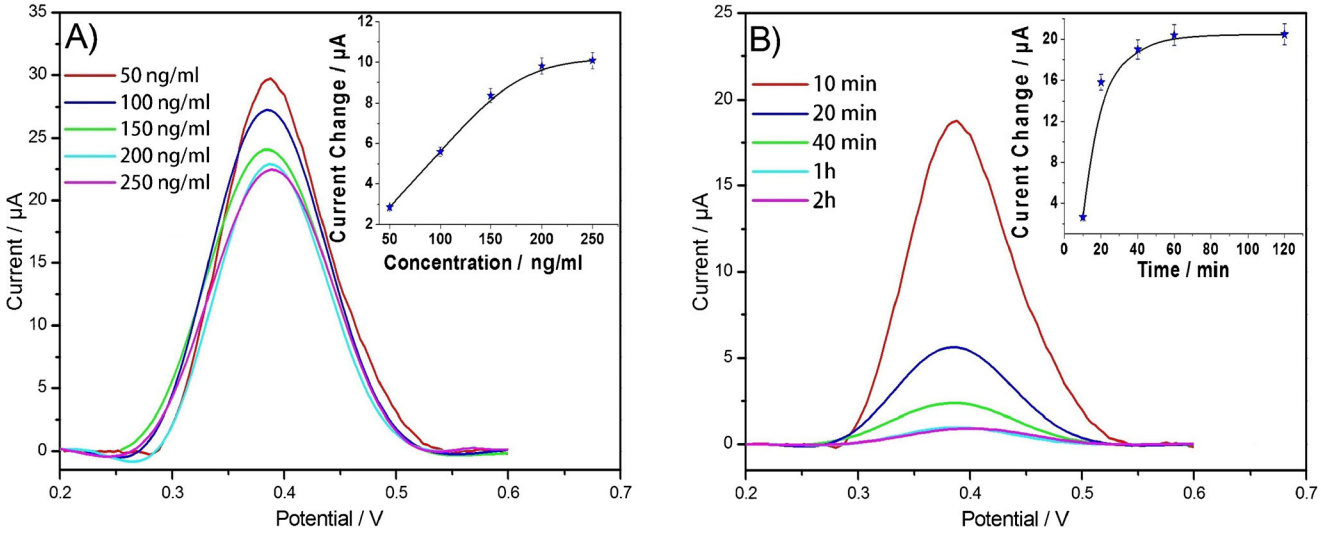


**Fig. 4** Differential pulse voltammetry scans obtained from the **a** optimization study of the concentration of amine-modified probes used for electrode modification ($n = 3$) and **b** the optimization study of the hybridization time of amine-modified probes and target sequences ($n = 3$).

pair of well-defined redox peaks was observed for all generations. The intensity of the oxidation–reduction peaks decreased with increase in the dendrimer generation, and was probably caused by the decreased electron transfer through dendrimer branches and increased distance of the ferrocene probe from the electrode surface. Further modification steps, which included ssDNA immobilization and the hybridization of complementary sequence (target DNA), were also characterized by CV. Figure 3b–d (G1, G2, and G3) shows that ssDNA immobilization and later hybridization of the target DNA caused a further decrease in the intensity of the current peaks coming from the ferrocene probe. To evaluate how different dendrimer generations perform in DNA hybridization detection, further experiments were performed with differential pulse voltammetry (DPV).

Before the analytical performance of the DNA biosensor was investigated, the ssDNA probe concentration and hybridization time were optimized. Figure 4a shows the results of the study performed to investigate the effect of different concentrations of the ssDNA sequence on the current response of the Au-Fc-PAMAM electrode. DPV was performed over the range from 0.2 to 0.6 V at an amplitude of 50 mV/s with the Au-Fc-PAMAM electrode, after which it was modified with amine-modified ssDNA probes of 50, 100, 150, 200, and 250 ng/ml concentration. The DPV current peak corresponding to ferrocene decreases as the amount of immobilized amine-modified probe increases. There was a linear increase in the current change until the concentration reached 150 ng/ml, after which the current difference slowly decreased (insert in Fig. 4a). This indicates that the maximum amount of the DNA probe had been immobilized on the electrode surface.

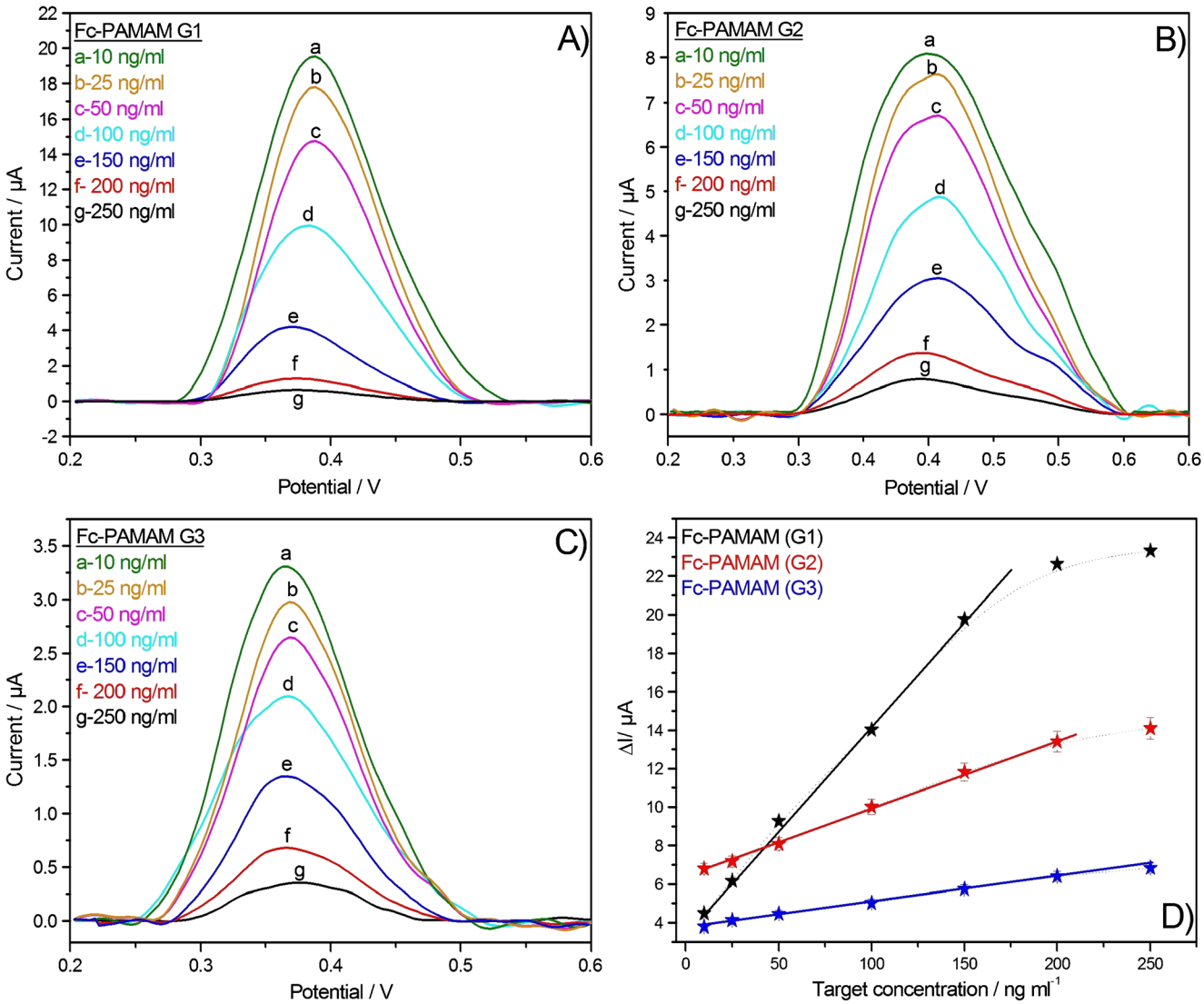


**Fig. 5** Differential pulse voltammetry measurements of different ferrocene-cored poly(amidoamine) (Fc-PAMAM) generations with different target DNA concentrations in the range from 10 to 250 ng/ml: **a** generation 1 (G1), **b** generation 2 (G2), and **c** generation 3 (G3). **d** Comparison of the calibration curves of DNA biosensing electrodes based on Fc-PAMAM G1, G2, and G3.

The reaction between Au-Fc-PAMAM/ssDNA and the target sequence requires an incubation period of a certain length, and because this time significantly affects the sensitivity and performance characteristics of the biosensing electrode, the optimum incubation time was determined as well (Fig. 4b). This set of experiments was performed by our recording DPV scans of the working electrode subjected to hybridization times of 10, 20, 40, 60, and 120 min. The response of the proposed DNA biosensor increased with the increase of the hybridization time until 40 min, after which it started to level off. Incubation of the electrode for 2 h resulted in no change in the DPV signal compared with 60 min, suggesting that complete hybridization of target DNA to the probe sequence had occurred. Therefore, 60 min was selected as the optimum hybridization time for the dendrimer-based electrode, which is similar to the time reported in the literature [32].

## Analytical characteristics of the DNA biosensor

The analytical performance of Au-Fc-PAMAM/ssDNA sensing electrodes was studied with target DNA with concentrations ranging from 10 to 250 ng/ml. Experiments were performed with electrodes modified with three different generations of Fc-PAMAM dendrimers: G1, G2, and G3. After incubation of the electrode in the target DNA solution, DPV was performed in the range from 0.2 to 0.6 V at a pulse amplitude of 50 mV/s in 50 mM phosphate-buffered saline (pH 7.4). Figure 5 illustrates a decrease in the redox current of the oxidation wave of ferrocene with increasing concentration of complementary DNA target. This variation in current intensity can be explained by the formation of double-stranded DNA (dsDNA) on the surface of the polymer membrane, which affects the electron transfer from the redox center to the surface. Basically, the blocking effect of dsDNA on the ionic transfer in the polymer membrane and also the effect of negatively charged DNA attached to the layer prevents the electron transfer from the redox center by electron hopping. Similar results were obtained in previous work in the case of polypyrrole associated with ferrocene [33–35]. Electrodes modified with G1 (Fig. 5a), G2 (Fig. 5b), and G3 (Fig. 5c) showed similar behavior, where the highest current peak was observed at a target DNA concentration of 10 ng/ml, after which the current decreased as the target DNA concentration increased, reaching the lowest current at 250 ng/ml. Although all the electrodes have similar behavior, the key difference is in the maximum current obtained after target DNA hybridization had been achieved. This is attributed to the dendrimer size, which dictates the distance of the ferrocene probe from the electrode surface [36] and also has a large impact on the overall response of the biosensor. This was also observed in

**Table 1** Comparison of the analytical performances of different previously reported electrodes with the proposed biosensor

| Electrode | Transducer | Linear range | Detection limit | Reference |
|---|---|---|---|---|
| ssDNA/$ZrO_2$/Au | DPV | 1–150 μg/ml | 0.065 μg/ml | [1] |
| MP/AuNP/SPCE | DPV | 0.01–10 μg/ml | 0.01 μg/ml | [40] |
| ODN/LDH | EIS | 18–270 ng/ml | 1.8 ng/ml | [41] |
| Single-stranded thiolated DNA/Ni/ZnO/ITO | DPV/EIS | 5–200 μg/ml | 5 μg/ml | [42] |
| ZnO/CNT nanocomposite | DPV/EIS | 5–180 μg/ml | 5 μg/ml | [43] |
| ssDNA/SH/Au electrode | CV | 10–60 μg/ml | NA | [2] |
| Au/PAMAM/CP | EIS | 0.1–100 nM | 0.033 nM | [25] |
| PAMAM(G4.5)/DNA | EIS | 0.1–100 nM | 2.5 pM | [26] |
| ds-DNA/PAMAM/REGO | DPV | 7–60 μM and 60–300 μM | 0.56 μM | [44] |
| MWCNT/PPy/PAMAM/Fc | SWV | 1 fM to 10 pM for DNAs<br>1–100 fM for $DNA_L$ | 0.3 fM | [20] |
| PAMAM (G1)/DNA/MB | DPV | 2 nM to 0.2 μM | 1 nM | [37] |
| GCE/PPI/AuNP | EIS | 0.01–5 nM | NA | [45] |
| Fc-PAMAM G1 | DPV | 10–150 ng/ml<br>1.3–20 nM | 2.9 ng/ml<br>0.38 nM | This work |
| Fc-PAMAM G2 | DPV | 10–200 ng/ml<br>1.3–26 nM | 7.02 ng/ml<br>0.92 nM | This work |
| Fc-PAMAM G3 | DPV | 10–230 ng/ml<br>1.3–33 nM | 5 ng/ml<br>0.66 nM | This work |

The detection limit is calculated by three times the standard deviation of the background signal divided by the sensitivity

*AuNP* gold nanoparticle, *CNT* carbon nanotube, *CP* capture probe, *CV* cyclic voltammetry, *DPV* differential pulse voltammetry, *EIS* electrochemical impedance spectroscopy, *Fc* ferrocene, *G1* generation 1, *G2* generation 2, *G3* generation 3, *G4.5* generation 4.5, *GCE* glassy carbon electrode, *ITO* indium tin oxide, *LDH* layered double hydroxide, *MB* methylene blue, *MP* magnetic particle, *MWCNT* multiwalled carbon nanotube, *NA* not available, *ODN* oligonucleotide, *PAMAM* poly(amidoamine), *PPI* poly(propyleneimine), *PPy* polypyrrole, *REGO* reduced graphene oxide, *SPCE* screen-printed carbon electrode, *ssDNA* single-stranded DNA, *SWV* square wave voltammetry, $DNA_S$ short chains of 15 bases, $DNA_L$ long chains of 75 bases

the calibration plot (Fig. 5d), which represents current change ($\Delta I$) versus concentration of target DNA, where $\Delta I$ was calculated as $\Delta I = I_{(\text{Fc-PAMAM(G1,G2,G3)/ssDNA})} - I_{(\text{Fc-PAMAM(G1,G2,G3)/ssDNA/target DNA})}$. Increase in the dendrimer generation could ideally provide more surface area for DNA probe immobilization; however, it also may reduce the ferrocene signal. As seen in Fig. 5d, the first generation of PAMAM had the highest $\Delta I$, which reflects the electrode's sensitivity, which is 0.13 μA/(ng/ml), almost several times higher than the sensitivity of G2 and G3. Increase in the target DNA concentration to 200 and 250 ng/ml resulted in very weak variation in the electrochemical signal. The linear regression equation and the correlation coefficient ($R$) for different generations of Fc-PAMAM are as follows:

G1: $\Delta I = 0.1078$[target DNA] + 3.5156, $R$= 0.9985;
G2: $\Delta I = 0.0366$[target DNA] + 6.3248, $R$= 0.9989;
G3: $\Delta I = 0.0133$[target DNA] + 3.7341, $R$= 0.9936.

All electrodes showed excellent performance in the detection of target DNA, with a wide linear range and low detection limits of 2.9 ng/ml (0.38 nM) for G1, 7.02 ng/ml (0.92 nM) for G2, and 5.0 ng/ml (0.66 nM) for G3. The electrode based on the first generation of PAMAM showed the highest sensitivity, 0.13 μA/(ng/ml). Table 1 presents a comparison of the analytical performances of the proposed electrodes with those of DNA biosensors based on different nanomaterials and dendrimers reported in previous studies. The proposed

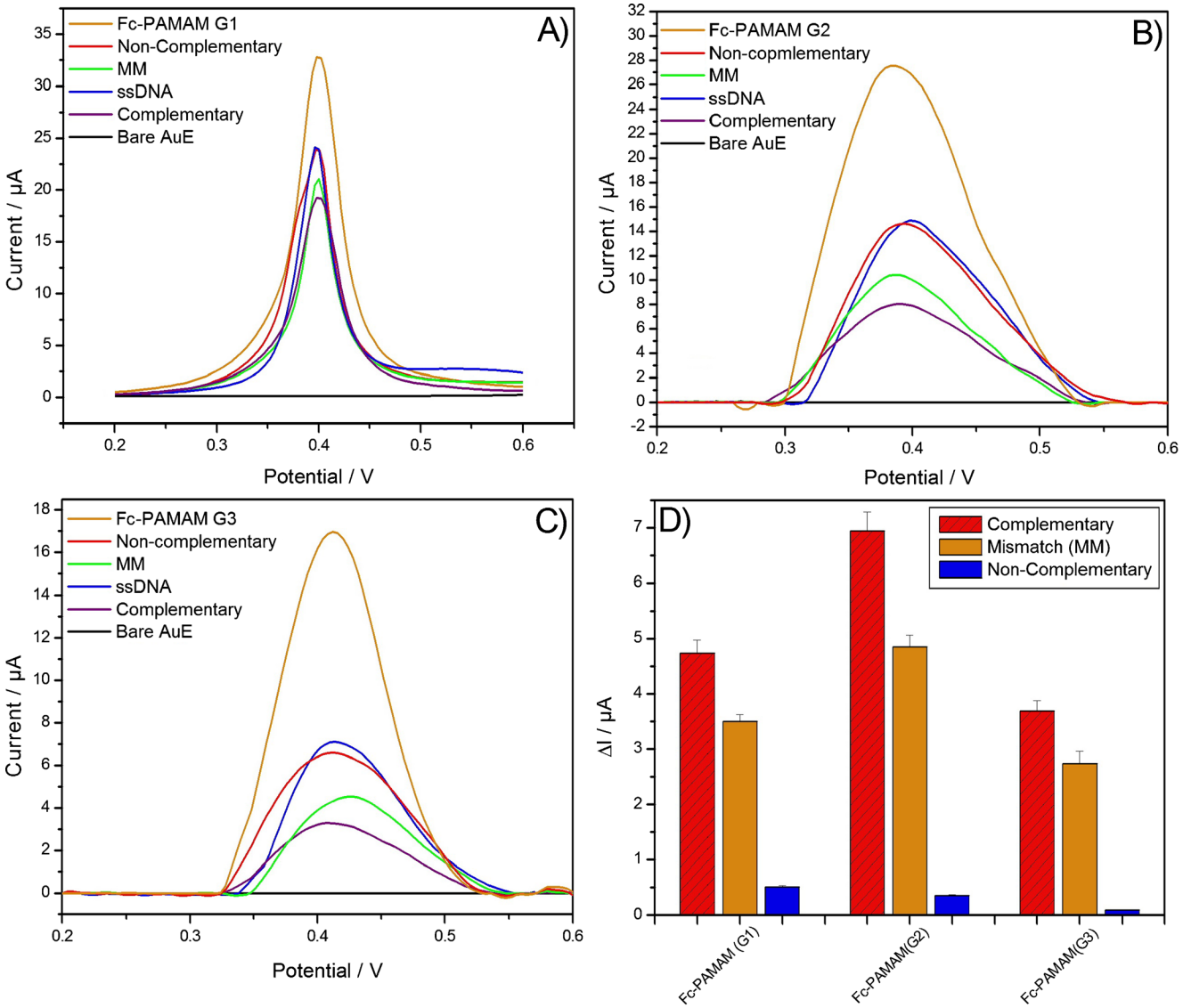


**Fig. 6** Differential pulse voltammetry scans from the selectivity study performed with electrodes based on ferrocene-cored poly(amidoamine) (Fc-PAMAM) generation 1 (G1) (**a**), generation 2 (G2) (**b**), and generation (G3) (**c**) incubated with different DNA sequences: complementary, noncomplementary, and one-base mismatch (MM). **d** Comparison of the current response of the biosensing electrodes used in the selectivity study. AuE gold electrode, ssDNA single-stranded DNA

biosensor exhibits better performance characteristics than most of the previously reported biosensors, and it introduces a new concept by integrating Fc-PAMAM for DNA-based biosensors.

In comparison with the previous detection strategy that used PAMAM dendrimer and methylene blue as the redox marker for DNA sensing [37], Fc-PAMAM is advantageous because incorporation of the redox marker into the dendrimer provides more persistent surface modification, resulting in better performance, such as a low detection limit. Different concentrations of methylene blue can influence the binding capacity of DNA, which adds an extra modification step to electrode fabrication, and thus could lead to less persistent surface modification. The biosensor is further compared with ferrocene-based electrochemical DNA biosensors such as the biosensor reported by Fan et al. [38], where the detection strategy involves ferrocene-tagged DNA stem-loop. The advantage of Fc-PAMAM over the aforementioned strategy is that the redox marker is always the same distance from the electrode, whereas in strategies based on ferrocene-tagged DNA stem-loop, the redox mediator position will change when target DNA hybridizes, which eventually leads to lower sensitivity on the order of nanoamperes and shifting of the redox peak toward higher potentials, whereas Fc-PAMAM sensitivity is on the order of microamperes and there is a stable redox peak with no shifting. The reported strategy is also advantageous in terms of the complexity of surface chemistry and cost of electrode preparation. For example, the detection strategy reported by Ren et al. [39] shows excellent detection performance, exhibiting high sensitivity and selectivity, but this strategy incorporates three monoclonal antibodies with attached DNA, which adds complexity to sensor preparation.

### Selectivity of the biosensor

The selectivity of the DNA biosensor was investigated by our recording variations in the intensity of the DPV current peaks using one-base-mismatch and noncomplementary DNA sequences. Figure 6 shows DPV plots of Au-Fc-PAMAM/ssDNA electrodes modified with G1 (Fig. 6a), G2 (Fig. 6b), and G3 (Fig. 6c), from which it can be observed that the highest peak current belongs to Fc-PAMAM. Further surface modification with ssDNA caused the signal to decrease, and hybridization of 20 ng target sequence per milliliter induced a large decrease in the recorded current. Further experiments were performed with noncomplementary sequences and demonstrated that the noncomplementary sequence is unable to hybridize with the ssDNA probe, resulting in negligible current change in all three generations. The same experiments were performed with a target DNA having one base mismatch that is a mutation observed in the *BRAC1* gene. The results show a decrease in the current but one that is not as big as when the complementary sequence is used. This indicates that the sequence is partially hybridized with the ssDNA probe. The same behavior was observed in all three Fc-PAMAM generations. Furthermore, overall comparison of the selectivity among the electrodes with different generations of Fc-PAMAM is shown in Fig. 6d. From this graph, it can be clearly seen that all proposed electrodes demonstrate high selectivity toward the target DNA, with interference of less than 5% from the noncomplementary sequence. Also, it can be see that the Fc-PAMAM/ssDNA electrode can clearly differentiate single-base mismatch in a DNA sequence from a complementary DNA sequence with approximately 37% current difference. These results indicate that Fc-PAMAM dendrimers are suitable for the fabrication of highly selective DNA biosensors for detection of single-base-mismatch mutation occurring in the *BARC1* gene.

## Conclusion

We reported the first electrochemical DNA biosensor using Fc-PAMAM dendrimers for cancer-susceptible-gene detection. Fabrication of the DNA biosensor was accomplished by our immobilizing ssDNA probe Fc-PAMAM dendrimer self-assembled on a Au electrode surface. The biosensor demonstrated excellent analytical performance, with a linear range of 10–150 ng/ml (1.3–20 nM), a low detection limit of 2.9 ng/ml (0.38 nM), and high sensitivity of 0.13 μA/(ng/ml). The linear range increases to 33 nM for the third generation of Fc-PAMAM (G3). The electrochemical DNA biosensor shows very good selectivity toward target DNA in the presence of single-base-mismatch and noncomplementary sequences. Furthermore, the biosensor exhibits excellent performance in differentiating a single-base-mismatch sequence from a noncomplementary sequence. The advantage of using Fc-PAMAM dendrimer over other reported dendrimers used in DNA biosensors is that the dendrimers are grown directly on ferrocene, which provides more persistent surface modification, resulting in better reproducibility and higher sensitivity. In terms of clinical utility, DNA biosensors will significantly decrease the time and increase the cost-effectiveness of a breast cancer diagnosis by shortening the time of sample pretreatment and analysis. This DNA biosensing approach looks promising for development of new DNA biosensors for fast and accurate breast cancer diagnosis.

**Acknowledgements** Some of this work was performed at the former Fatih University as a part of the work presented in FK's master thesis.

### Compliance with ethical standards

**Conflict of interest** The authors declare that they have no competing interests.

## References


1. Das M, Sumana G, Nagarajan R, Malhotra BD. Zirconia based nucleic acid sensor for Mycobacterium tuberculosis detection. Appl Phys Lett. 2010;96(13):133703. https://doi.org/10.1063/1.3293447.
2. Patel MK, Solanki PR, Kumar A, Khare S, Gupta S, Malhotra BD. Electrochemical DNA sensor for Neisseria meningitidis detection. Biosens Bioelectron. 2010;25(12):2586–91. https://doi.org/10.1016/j.bios.2010.04.025.
3. Liu S, Su W, Li Z, Ding X. Electrochemical detection of lung cancer specific microRNAs using 3D DNA origami nanostructures. Biosens Bioelectron. 2015;71:57–61. https://doi.org/10.1016/j.bios.2015.04.006.
4. Rasheed PA, Sandhyarani N. Graphene-DNA electrochemical sensor for the sensitive detection of BRCA1 gene. Sens Actuators B. 2014;204:777–82. https://doi.org/10.1016/j.snb.2014.08.043.
5. Borghei Y-S, Hosseini M, Ganjali MR, Ju H. A unique FRET approach toward detection of single-base mismatch DNA in BRCA1 gene. Mater Sci Eng C. 2019;97:406–11. https://doi.org/10.1016/j.msec.2018.12.049.
6. Wang Y, Huang X, Li H, Guo L. Sensitive impedimetric DNA biosensor based on (Nb,V) codoped TiO2 for breast cancer susceptible gene detection. Mater Sci Eng C. 2017;77:867–73. https://doi.org/10.1016/j.msec.2017.03.260.
7. World Health Organization. Cancer. https://www.who.int/news-room/fact-sheets/detail/cancer (2018).
8. Sifri R, Gangadharappa S, Acheson LS. Identifying and testing for hereditary susceptibility to common cancers. CA Cancer J Clin. 2004;54(6):309–26. https://doi.org/10.3322/canjclin.54.6.309.
9. Chen L, Liu X, Chen C. Impedimetric biosensor modified with hydrophilic material of tannic acid/polyethylene glycol and dopamine-assisted deposition for detection of breast cancer-related BRCA1 gene. J Electroanal Chem. 2017;791:204–10. https://doi.org/10.1016/j.jelechem.2017.03.001.
10. Godet I, Gilkes DM. BRCA1 and BRCA2 mutations and treatment strategies for breast cancer. Integr Cancer Sci Ther. 2017;4(1). https://doi.org/10.15761/icst.1000228.
11. Coleman MP, Quaresma M, Berrino F, Lutz J-M, De Angelis R, Capocaccia R, et al. Cancer survival in five continents: a worldwide population-based study (CONCORD). Lancet Oncol. 2008;9(8):730–56. https://doi.org/10.1016/S1470-2045(08)70179-7.
12. Jaure O, Alonso EN, Braico DA, Nieto A, Orozco M, Morelli C, et al. BRCA1 polymorphism in breast cancer patients from Argentina. Oncol Lett. 2015;9(2):845–50. https://doi.org/10.3892/ol.2014.2772.
13. Wang J. Electrochemical biosensors: towards point-of-care cancer diagnostics. Biosens Bioelectron. 2006;21(10):1887–92. https://doi.org/10.1016/j.bios.2005.10.027.
14. Amer WA, Wang L, Amin AM, Ma L, Yu H. Recent progress in the synthesis and applications of some ferrocene derivatives and ferrocene-based polymers. J Inorg Organomet Polym Mater. 2010;20(4):605–15. https://doi.org/10.1007/s10904-010-9373-6.
15. Fabre B. Ferrocene-terminated monolayers covalently bound to hydrogen-terminated silicon surfaces. toward the development of charge storage and communication devices. Acc Chem Res. 2010;43(12):1509–18. https://doi.org/10.1021/ar100085q.
16. Dervisevic E, Dervisevic M, Nyangwebah JN, Şenel M. Development of novel amperometric urea biosensor based on Fc-PAMAM and MWCNT bio-nanocomposite film. Sens Actuators B. 2017;246:920–6. https://doi.org/10.1016/j.snb.2017.02.122.
17. Şenel M, Abasıyanık MF. Construction of a novel glucose biosensor based on covalent immobilization of glucose oxidase on poly(glycidyl methacrylate-co-vinylferrocene). Electroanalysis. 2010;22(15):1765–71. https://doi.org/10.1002/elan.200900644.
18. Miodek A, Mejri-Omrani N, Khoder R, Korri-Youssoufi H. Electrochemical functionalization of polypyrrole through amine oxidation of poly(amidoamine) dendrimers: application to DNA biosensor. Talanta. 2016;154:446–54. https://doi.org/10.1016/j.talanta.2016.03.076.
19. Dervisevic M, Senel M, Sagir T, Isik S. Boronic acid vs. folic acid: a comparison of the bio-recognition performances by impedimetric cytosensors based on ferrocene cored dendrimer. Biosens Bioelectron. 2017;91:680–6. https://doi.org/10.1016/j.bios.2017.01.030.
20. Miodek A, Mejri N, Gomgnimbou M, Sola C, Korri-Youssoufi H. E-DNA sensor of Mycobacterium tuberculosis based on electrochemical assembly of nanomaterials (MWCNTs/PPy/PAMAM). Anal Chem. 2015;87(18):9257–64. https://doi.org/10.1021/acs.analchem.5b01761.
21. Hasanzadeh M, Shadjou N, Eskandani M, Soleymani J, Jafari F, de la Guardia M. Dendrimer-encapsulated and cored metal nanoparticles for electrochemical nanobiosensing. Trends Anal Chem. 2014;53:137–49. https://doi.org/10.1016/j.trac.2013.09.015.
22. Bahadır EB, Sezgintürk MK. Poly(amidoamine) (PAMAM): an emerging material for electrochemical bio(sensing) applications. Talanta. 2016;148:427–38. https://doi.org/10.1016/j.talanta.2015.11.022.
23. D A Tomalia, H Baker, J Dewald, M Hall, G Kallos, S Martin, J Roeck, J Ryder, P Smith, (1985) A New Class of Polymers: Starburst-Dendritic Macromolecules. Polymer Journal 17 (1):117-132
24. Koc FE, Senel M. Solubility enhancement of non-steroidal anti-inflammatory drugs (NSAIDs) using polypolypropylene oxide core PAMAM dendrimers. Int J Pharma. 2013;451(1-2):18–22. https://doi.org/10.1016/j.ijpharm.2013.04.062.
25. Li Q, Yu C, Gao R, Xia C, Yuan G, Li Y, et al. A novel DNA biosensor integrated with polypyrrole/streptavidin and Au-PAMAM-CP bionanocomposite probes to detect the rs4839469 locus of the vangl1 gene for dysontogenesis prediction. Biosens Bioelectron. 2016;80:674–81. https://doi.org/10.1016/j.bios.2016.02.025.
26. Zhu N, Gao H, Gu Y, Xu Q, He P, Fang Y. PAMAM dendrimer-enhanced DNA biosensors based on electrochemical impedance spectroscopy. Analyst. 2009;134(5):860-6. d https://doi.org/10.1039/B815488K.
27. Kavosi B, Salimi A, Hallaj R, Moradi F. Ultrasensitive electrochemical immunosensor for PSA biomarker detection in prostate cancer cells using gold nanoparticles/PAMAM dendrimer loaded with enzyme linked aptamer as integrated triple signal amplification strategy. Biosens Bioelectron. 2015;74:915–23. https://doi.org/10.1016/j.bios.2015.07.064.
28. Borisova B, Sánchez A, Jiménez-Falcao S, Martín M, Salazar P, Parrado C, et al. Reduced graphene oxide-carboxymethylcellulose layered with platinum nanoparticles/PAMAM dendrimer/magnetic nanoparticles hybrids. Application to the preparation of enzyme electrochemical biosensors. Sens Actuators B. 2016;232:84–90. https://doi.org/10.1016/j.snb.2016.02.106.
29. Dervisevic M, Dervisevic E, Şenel M. Design of amperometric urea biosensor based on self-assembled monolayer of cystamine/PAMAM-grafted MWCNT/Urease. Sens Actuators B. 2018;254:93–101. https://doi.org/10.1016/j.snb.2017.06.161.
30. Dervisevic M, Dervisevic E, Senel M, Cevik E, Yildiz HB, Camurlu P. Construction of ferrocene modified conducting polymer based amperometric urea biosensor. Enzyme Microb Technol. 2017;102:53–9. https://doi.org/10.1016/j.enzmictec.2017.04.002.
31. Sağır T, Işık S, Şenel M. Ferrocene incorporated PAMAM dendrons: synthesis, characterization, and anti-cancer activity against AGS cell line. Med Chem Res. 2013;22(10):4867–76. https://doi.org/10.1007/s00044-013-0491-x.

32. Li A, Yang F, Ma Y, Yang X. Electrochemical impedance detection of DNA hybridization based on dendrimer modified electrode. Biosens Bioelectron. 2007;22(8):1716–22. https://doi.org/10.1016/j.bios.2006.07.033.
33. Bizid S, Blili S, Mlika R, Haj Said A, Korri-Youssoufi H. Direct electrochemical DNA Sensor based on a new redox oligomer modified with ferrocene and carboxylic acid: application to the detection of Mycobacterium tuberculosis mutant strain. Anal Chim Acta. 2017;994:10–8. https://doi.org/10.1016/j.aca.2017.09.022.
34. Bizid S, Mlika R, Haj Said A, Chemli M, Korri Youssoufi H. Investigations of poly(p-phenylene) modified with ferrocene and their application in electrochemical DNA sensing. Sens Actuators B. 2016;226:370–80. https://doi.org/10.1016/j.snb.2015.11.137.
35. Kuralay F, Erdem A, Abacı S, Özyörük H, Yıldız A. Poly(vinylferrocenium) coated disposable pencil graphite electrode for DNA hybridization. Electrochem Commun. 2009;11(6):1242–6. https://doi.org/10.1016/j.elecom.2009.04.010.
36. Steentjes T, Jonkheijm P, Huskens J. Electron transfer processes in ferrocene-modified poly(ethylene glycol) monolayers on electrodes. Langmuir. 2017;33(43):11878–83. https://doi.org/10.1021/acs.langmuir.7b02160.
37. Wei-Jie S, Shi-Yun A, Jin-Huan L, Lu-Sheng Z. Electrochemical biosensor based on dendrimer immobilized deoxyribonucleic acid. Chin J Anal Chem. 2008;36(3):335–8. https://doi.org/10.1016/S1872-2040(08)60025-0.
38. Fan C, Plaxco KW, Heeger AJ. Electrochemical interrogation of conformational changes as a reagentless method for the sequence-specific detection of DNA. Proc Natl Acad Sci U S A. 2003;100(16):9134–7. https://doi.org/10.1073/pnas.1633515100.
39. Ren K, Wu J, Ju H, Yan F. Target-driven triple-binder assembly of MNAzyme for amplified electrochemical immunosensing of protein biomarker. Anal Chem. 2015;87(3):1694–700. https://doi.org/10.1021/ac504277z.
40. Torres-Chavolla E, Alocilja EC. Nanoparticle based DNA biosensor for tuberculosis detection using thermophilic helicase-dependent isothermal amplification. Biosens Bioelectron. 2011;26(11):4614–8. https://doi.org/10.1016/j.bios.2011.04.055.
41. Baccar ZM, Caballero D, Eritja R, Errachid A. Development of an impedimetric DNA-biosensor based on layered double hydroxide for the detection of long ssDNA sequences. Electrochim Acta. 2012;74:123–9. https://doi.org/10.1016/j.electacta.2012.04.031.
42. Tak M, Gupta V, Tomar M. An electrochemical DNA biosensor based on Ni doped ZnO thin film for meningitis detection. J Electroanal Chem. 2017;792:8–14. https://doi.org/10.1016/j.jelechem.2017.03.032.
43. Tak M, Gupta V, Tomar M. A ZnO–CNT nanocomposite based electrochemical DNA biosensor for meningitis detection. RSC Adv. 2016;6(80):76214–22. https://doi.org/10.1039/C6RA12453D.
44. Hatamluyi B, Es'haghi Z. Quantitative biodetection of anticancer drug Rituxan with DNA biosensor modified PAMAM dendrimer/reduced graphene oxide nanocomposite. Electroanalysis. 2018;30(8):1659–68. https://doi.org/10.1002/elan.201800014.
45. Arotiba O, Owino J, Songa E, Hendricks N, Waryo T, Jahed N, et al. An electrochemical DNA biosensor developed on a nanocomposite platform of gold and poly(propyleneimine) dendrimer. Sensors (Basel). 2008;8(11):6791–809. https://doi.org/10.3390/s8116791.